Online Appendix for "Drifts and Volatilities under Measurement Error: Assessing Monetary Policy Shocks over the Last Century"

Pooyan Amir-Ahmadi   Christian Matthes
Mu-Chun Wang [*]

November 11, 2015

1 Data

1.1 Annual Output Growth

Our output growth series is obtained by splicing two different real output series covering different time spans. We use real GNP series as constructed by Balke & Gordon (1986) from the first quarter of 1876 to the fourth quarter of 1946 (1930:Q1 and 1947:Q1 are the break dates for the parameters of the measurement error process associated with this series). Starting in 1947:Q1, we use the real GDP series provided by the St. Louis Fed FRED database covering the first quarter of 1947 to the second quarter of 2011. The spliced series are transformed in logs and then we take year-on-year differences.

1.2 Annual Inflation Rate

The corresponding annual inflation rate is also based on the combination of two different series on the output deflator. Again the first part comes from Balke & Gordon (1986) covering the period 1876Q1-1946Q4. Just as with output growth, the break date for the parameters of the measurement error process is 1947:Q1. The second part of the series comes

from the St. Louis Fed FRED database covering the time span 1948Q1-2011Q2. Again we transform the data into year-on-year growth rates.

1.3 Short-Term Interest Rate

The short term interest rate plays the role of a potential direct or indirect monetary policy instrument for at least a substantial part of the time span we analyze. There is no single series on shorter interest rates at quarterly frequency for the full sample, which requires constructing a series based on several data sources reflecting short-term borrowing conditions. From 1920Q1-2011Q2 we use data on the 90-day T-Bill rate from the secondary market. Prior to that we backcast the series including as regressors data on call money rates and commercial paper rates. These two series show a strong contemporaneous correlation with the T-Bill rate when all series are available. The series used for backcasting and our target short term interest rate series are all available at monthly frequency. Specifically, we regress 90-day T-Bill rate on call money rates and commercial paper rates based on a sample running from February 1920 to April 1934[1]. Combining the resulting coefficients with our regressors we can backcast our target series back to the first quarter of 1876. This way we interpolate backward the missing observations for the 90-day T-Bill rate. We thus avoid using the six-month short term interest rate, which would lead to a maturity mismatch combining the three-month and six-month rates. Furthermore, we prefer the shorter maturity rate as a potential monetary policy instrument. We use annualized interest rates throughout. The break point for the parameters of the measurement error process is 1920:Q1.

1.4 Long-Term Interest Rate

As for the term spread, we employ the difference between a constructed measure of the long-term interest rate and the short-term interest rate described in the previous section. The lack of a consistent long-term government benchmark interest rate requires the combination and backcasting of three indicators. From 1920Q1-2011Q2 we use data on the 10-year government bond yields at constant maturities. Prior to that, we backcast the series including as regressors data on railroad bond yields (high grade) and a railroad bond yields index. Again, there is a strong contemporaneous correlation between the series we use to approximate the long-term interest rate and that interest rate itself when all series are available.

We regress 10-year government bond yields at constant maturities on

---

[1]Some experimentation with alternative windows for the backcasting exercise lead to essentially same results.

railroad bond yields (high grade) and railroad bond yields index based on a sample running from February 1920 to April 1934. Combining the resulting coefficients with our regressors we can backcast our target series back to the first quarter in 1876. The long-term interest rate is expressed in annual terms. Just as with short-term rates, the break point for the parameters of the measurement error process here is 1920:Q1.

1.5 Annual Base Money Growth

The monetary base measure we use to represent a direct or indirect monetary policy instrument is obtained by combining by two series. The first part of the sample from 1876Q1-1958Q4 comes from Balke & Gordon (1986) and the second part from the FRED database covering 1959Q1-2011Q2. Since the Balke & Gordon (1986) data uses different sources itself, we allow for further breaks in 1918 and 1935 in addition to the break point in 1958.[2]

2 Prior Choice

We choose priors in a way to stay as close as possible to the previous literature, while taking into account our larger sample and the addition of measurement error processes. We use data from 1876:Q1 to 1913:Q4 to initialize the priors for the VAR for y_t by using a fixed coefficient VAR, similarly to Primiceri (2005).

The priors for the measurement errors and the associated parameters are set similarly to Cogley, Sargent & Surico (2015). The priors are the same for each data source, but vary across variables to take into account the different volatilities of each variable.

We use independent normal-inverse gamma priors for each set of measurement error process coefficients. As we change the measurement error process for inflation and output growth, we keep the structure of the prior (i.e. the distributional assumptions), but modify some of the parameters of the priors for the measurement error processes to take into account how the measurement error enters the measurement equations for inflation and output growth. The prior for the AR coefficients for the measurement errors is independent across variables and break dates. It is Gaussian with mean 0 and prior standard deviation 0.45, which we keep

---

[2]While the measurement of the money base has undergone multiple changes over the years, our reading of St. Louis Fed documentation on this subject helped us identify these possibly major break points. The St Louis Fed uses similar sources for the first part of the sample as do Balke & Gordon (1986). Links to this documentation are:

1. http://research.stlouisfed.org/publications/review/03/09/Anderson.pdf

2. http://research.stlouisfed.org/aggreg/newbase.html

for both sets of specifications, our benchmark specification and the specification with $M_i(L) = 1 \forall i$. The prior for the variance of the innovation of the AR processes is inverse-gamma and independent across variables and break dates. The mode of the inverse-gamma distribution is set to a fraction of the standard deviation of each variable during the training sample (the prior scale parameters are set to 2). Cogley, Sargent & Surico (2015) use 50 % of the training sample standard deviation for the prior mode for their model of inflation. For our growth rate specification (which is the specification Cogley, Sargent & Surico (2015) used for their model of inflation), we use the same value for our inflation measurement error as well as for the interest rate and spread series, but found that the standard deviation for real GDP growth and money growth during the training sample is so high that mechanically using the same value as Cogley, Sargent & Surico (2015) for those series resulted in somewhat implausible estimates. Instead of a scaling factor of 50 % of the training standard deviation, we in that case thus a scaling factor of 15 % of the training sample deviation for GDP growth and money growth. Since we use priors for σ_j^i with an infinite variance (Cogley, Sargent & Surico (2015) also use a prior with infinite variances for their corresponding parameter), this change does not restrict the posterior to assign only a minor role to measurement error.

For our benchmark specification, we keep the prior on the AR coefficients, but reduce the prior mode for the innovation in the AR process. We do this because the level specification automatically introduces additional volatility (this is easiest to see if we think of iid measurement errors in levels - then the composite measurement error is the difference of two iid measurement errors and thus has twice the volatility of the original measurement error). We thus set the prior mode of the innovation volatilities in the measurement error processes to capture half of the standard deviation that the corresponding prior in the growth rate specification captured. We keep the scale parameters the same across the two specifications. Summarizing the priors for the measurement error process, we have

$$\rho_j^i \sim N(0, .45^2) \tag{1}$$

$$\sigma_j^i \sim IG(scaling_i * \hat{\sigma}_{i,train}^2, 2) \tag{2}$$

where $\hat{\sigma}_{i,train}^2$ is the estimate of the variance of observed variable i from the training sample and scaling is set as described above. We use (somewhat non-standard) notation for the inverse gamma where the first argument gives the prior mode and the second argument the scale parameter.[3]

An important prior for time-varying parameter VARs is the prior for

---

[3]The scale parameter of an inverse gamma distribution is one of the two parameters commonly used for this family of distributions. Importantly, when we talk about the scale parameter, we do not mean $scaling_i$.

Q, the covariance matrix of the residuals that enter the law of motion for θ. We assume that Q, which governs the amount of time variation in the VAR coefficients, follows an inverse Wishart distribution with the following parameters:

$$Q \sim IW(\kappa_Q^2 * 152 * V(\theta_{OLS}), 152) \tag{3}$$

where the prior degrees of freedom is set to 152, which is the length of our training sample, $V(\theta_{OLS})$ is the variance of the OLS estimator of the VAR coefficients in our training sample and $\kappa_Q = 0.01$ is the tuning parameter to parameterize the prior belief about the amount of time variation. Primiceri (2005) uses exactly the same approach to set his prior. Choosing the same approach allows us to keep our results comparable to his. The other priors are also set according to Primiceri (2005), adjusting for the larger size of our vector of observables. In contrast to Cogley & Sargent (2005), we do not impose the prior that the companion matrix of our VAR only has eigenvalues smaller than 1 in absolute value. We do this to be able to study if there is significant variation in the probability of this local non-stationarity.

3 Sources of Volatility

Volatility in time series models can be traced back to two sources: the innovations (or unpredictable components) that influence the time series of interest and the systematic response to those innovations. To make this point, consider a univariate AR(1) model with Gaussian innovations:

$$z_t = \rho z_{t-1} + w_t, \, w_t \sim N(0, \sigma_w^2) \tag{4}$$

Then the j-step ahead conditional variance is given by

$$Var_t(z_{t+j}) = \sigma_w^2 \sum_{k=1}^{j} \rho^{2(j-k)} \tag{5}$$

We can see that the volatility of this process is fully characterized by the autoregressive coefficient and the variance of the innovation. The next two sections present a similar characterization for our time-varying VAR. The objects corresponding to ρ in the multivariate context are the $\mathbf{A}_t$ matrices, which are high dimensional. To study dynamics, we can focus on the eigenvalues, but even those are large in number (given that they vary over time). The section below therefore focuses on the largest eigenvalue in absolute value. This object does not fully characterize the effects of time variation in persistence on volatility, but it does give an idea about whether or not our estimated model features (locally) unstable dynamics, which in turn will have an effect on volatility.

3.1 Are There Explosive Dynamics in U.S. Time Series?

We study the probability of matrix $\mathbf{A}_t$ having eigenvalues larger than 1 in our sample by checking the draws of $\mathbf{A}_t$ that are generated by our Gibbs sampler. We can do this because, as mentioned before, we do not follow Cogley & Sargent (2005) and impose conditions on the eigenvalues of the companion matrix of our VAR. The right panel of Figure 1 shows this probability, whereas the left panel shows draws from the posterior path of the maximum absolute eigenvalue as well as the median and 68 percent posterior probability bands.
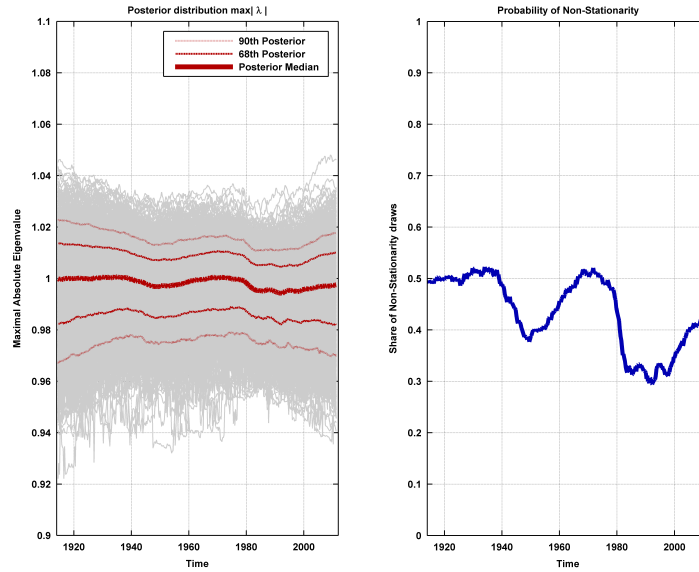

Figure 1: Explosive behavior

The average level of the probability until the 1940s is quite high, reaching over 0.5. The probability drops almost 20 percentage points at the end of WWII. It rises again until the end of the 1970s. The second big decrease in this probability following the Volcker disinflation could be interpreted in terms of a structural model in which agents have to learn about the true data-generating process (DGP): Cogley, Matthes & Sbordone (2015) show that times in which beliefs of private agents are far away from the DGP can lead to explosive dynamics, whereas the probability of explosive eigenvalues falls as beliefs move closer to the true DGP. An alternative structural model that can give temporarily explosive dynamics is given by Bianchi & Ilut (2013). To wit, we find two large changes in the probability of local non-stationarity.

Despite the fact that high probability of explosiveness can be found in various periods in the history, the left panel of Figure 1 shows that the

absolute value of those eigenvalues larger than 1 is only slightly larger than 1. This means that even if there are eigenvalues larger than 1, it takes a long time for the economy to become noticeably unstable. Concerning the kind of stationarity restrictions used by Cogley & Sargent (2005), there is a substantial posterior probability of having explosive eigenvalues, making estimation algorithms with this restriction slow to converge. At the same time, the restriction itself is not far from being met for large parts of post-WWII data in the sense that the estimated eigenvalues are not far from 1[4].

4   The Growth Rate Specification for Measurement Error

In this section we study a model with $M_i(L) = 1 \, \forall i$. The differences in results between this approach and our benchmark are small. For the sake of brevity, we focus on the estimated 'true' data as well as impulse responses. The first figure shows the estimated 'true' data (with the median in bold red), and 68% posterior bands. The break points for the measurement errors are the same as for our benchmark, with the exception that we do not have a break for GDP growth in 1930. Adding this break here does not change the results. After the last break point the estimated 'true' data coincides with the observed data. We see in figure 2 that the estimated 'true'data is very similar to that obtained using our benchmark specification. The major difference between this specification and our benchmark is that this specification attributes the GDP growth downturns in the second half of the 1930s and after WWII to movements in actual data, whereas our benchmark mainly sees this as measurement error.

Concerning the impulse responses, the patterns are very similar to our benchmark results. Figures 3 and 4 shoes the impulse responses. Once thing we do find in this specification, at least in the one standard deviation shock case, is a change in the behavior of the GDP growth impulse response with the Fed Treasury Accord, in line with some of the reduced form changes that we found both in the benchmark case and with this specification.

Table 1 shows the volatility of the estimated and observed GDP growth series for different periods. We see the same patterns as for our benchmark specification. The reduction in the volatility of the estimated 'true' series starting in 1930 is still present, albeit less pronounced.

---

[4]Given that we also use pre-WWII data, this approach would be harder to defend for our application.
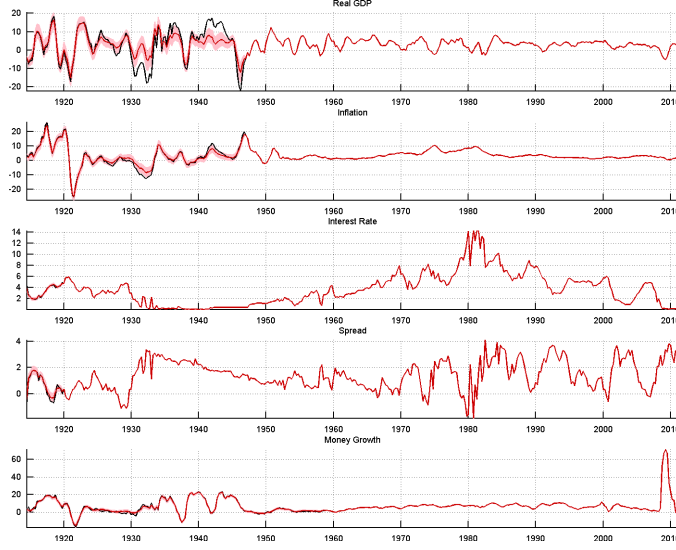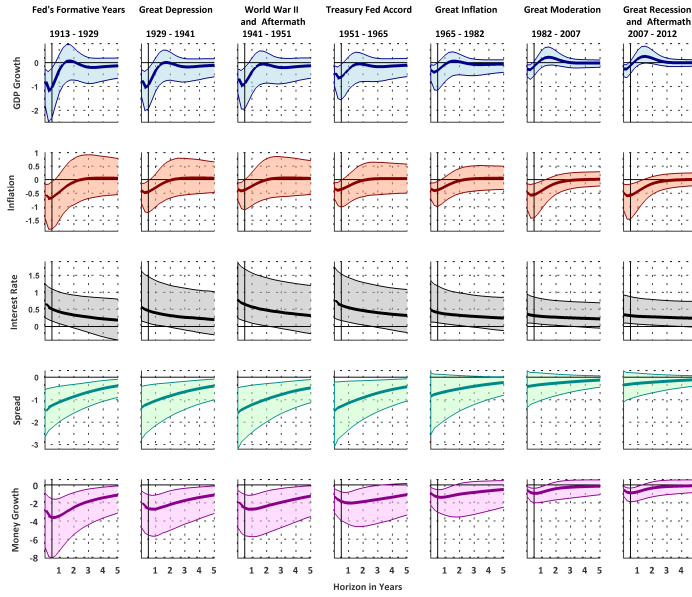
Figure 2: Data

Figure 3: Impulse responses for one standard deviation shock

5   Estimation Algorithm

We use a Gibbs-Sampler to approximate the posterior distribution by generating $100,000$ draws. The exact implementation for time-varying parameters and stochastic volatilities follows Primiceri (2005) including the corrigendum of Del Negro and Primiceri (2013). In addition, we propose a multivariate generalization of Cogley, Sargent & Surico (2015) to simulate the posterior distribution for measurement error process parameters and unobserved 'true' data.
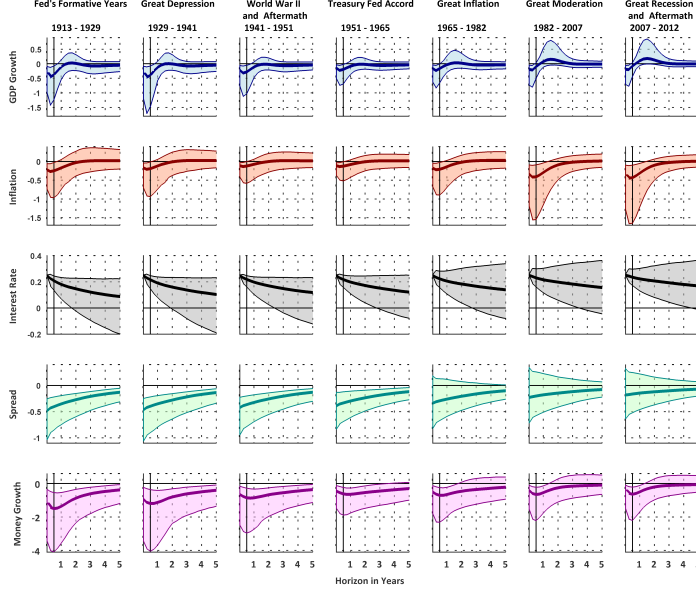
Figure 4: Impulse responses for 25 basis point nominal interest rate shock

	Estimated	Observed	Estimated Post WWII	Observed Post WWII
1915-1946	6.1	9.6	2.4	3.7
1915-1929	6.7	7.7	2.6	2.9
1930-1946	5.5	11.0	2.1	4.2
1947-2006	2.6	2.6	1	1

Table 1: Standard deviation of observed and estimated real GDP growth for different periods calculated using the alternative specification of the measurement error process.

Let $\tilde{y}^T$ be the observed noisy data vector, $S^T = (y^T, m^T)$ be the vector of the unobserved data and associated measurement errors with and Θ^T be the collection of all parameters of the time-varying VAR with stochastic volatilities. Note that conditional on the (partly unobserved) 'true' data, the steps we borrow from Primiceri (2005) do not need to be altered: knowledge of the measurement error or the parameters of the measurement error process are irrelevant for those steps in the Gibbs sampler. The algorithm proceeds as follows[5]

1. Draw Σ^T from $p(\Sigma^T | y^T, \theta^T, \Lambda^T, V, s^T)$. This step requires us to generate draws from a nonlinear state space system. We use the approach by Kim, Shephard & Chib (1998) to approximate draws from the desired distribution. For a correct posterior sampling of the stochastic volatilities we follow the corrigendum in Del Negro and Primiceri

---

[5]A superscript T denotes a sample of the relevant variable from $t = 1$ to T.

9

(2013) and the modified steps therein.

2. Draw θ^T from $p(\theta^T|y^T, \Lambda^T, \Sigma^T, V)$. Conditional on all other parameter blocks equations (4) and (5) from the main text form a linear Gaussian state space system. This step can be carried out using the simulation smoother detailed in Carter & Kohn (1994).

3. Draw Λ^T from $p(\Lambda^T|y^T, \theta^T, \Sigma^T, V)$. Again we draw these covariance states based on the simulation smoother of the previous step, exploiting our assumption that the covariance matrix of the innovations in the law of motion for the λ coefficients is block diagonal. This assumption follows Primiceri (2005), where further details on this step can be found.

4. Draw V from $p(V|\Sigma^T y^T, \theta^T, \Lambda^T)$. Given our distributional assumptions, this conditional posterior of the time-invariant variances follows an inverse-Wishart distribution, which we can easily sample from.

5. Draw S^T from $p(S^T|\Theta^T, \rho_m, \sigma_m^2, \tilde{y}^T)$

   Conditional on $\Theta^T, \rho_m, \sigma_m^2$ and $\tilde{y}^T$, equation (2) from the main text and and the set of equations (10) from the main text form a linear-Gaussian state-space system where the conditional posterior of S^T is also Gaussian and can be simulated using the Carter & Kohn (1994) sampler. The initialization of the Kalman filter is given by

$$S_0 = \begin{pmatrix} y_0 \\ m_0 \end{pmatrix} = \begin{pmatrix} \bar{y}_{train} \\ 0 \end{pmatrix}$$

   where $\bar{y}_{train}$ is the mean of the training sample of the observed data vector $\tilde{y}^T$. The initial MSE matrix P_0 is specified as

$$P_0 = \begin{pmatrix} \hat{\sigma}_{1,train}^2 & 0 & 0 & \cdots & 0 & 0 \\ 0 & \ddots & 0 & 0 & 0 & 0 \\ \vdots & 0 & \hat{\sigma}_{M,train}^2 & 0 & 0 & \vdots \\ 0 & 0 & 0 & \sigma_{1,\text{mode}}^2 & 0 & 0 \\ 0 & 0 & 0 & 0 & \ddots & 0 \\ 0 & 0 & 0 & \cdots & 0 & \sigma_{M,\text{mode}}^2 \end{pmatrix}$$

   where $\hat{\sigma}_{i,train}^2$ is the unbiased variance estimate of the observed variable i from the training sample and $\sigma_{i,\text{mode}}^2$ is the prior mode of the variance of the measurement error i. We describe the state space system used to draw S in more detail in a separate section below.

6. Draw ρ_m and σ_m^2 from $p(\rho_m, \sigma_m^2|S^T, \Theta^T, \tilde{y}^T)$

Since all measurement error innovations are independent, the only relevant conditional information set is m^T. Conditioned on m^T and using the independent normal-inverse gamma prior for each of the measurement error process independently, the conditional posterior $p(\rho_m|\sigma_m^2, m^T)$ is normal and the conditional posterior $p(\sigma_m^2|\rho_m, m^T)$ is inverse gamma, which can be sampled using two Gibbs steps.

7. Draw s^T, the sequence of indicators for the mixture of normals needed for the Kim et al. (1998) stochastic volatility algorithm.

6 Algorithm to Draw Generalized Impulse Responses

Here we describe the Monte Carlo procedure for the identification of the evolving generalized impulse response functions to contractionary monetary policy shocks employed via pure sign restrictions as briefly outlined in the main text. The exposition draws mostly on the procedure described in Benati & Mumtaz (2007), Baumeister & Benati (2013) and Baumeister & Peersman (2013), who build on Koop, Pesaran & Potter (1996).

We compute the candidate generalized impulse responses as the difference between the conditional expectations with and without a specific value of the exogenous shock ϵ at time t

$$irf_{cand,t+k} = E[X_{t+k} \mid \epsilon_t, \omega_t] - E[X_{t+k} \mid \omega_t]$$

where X_{t+k} contains the forecasts of the endogenous variables at horizon k, ω_t represents the current information set that captures the entire history up to that point in time, and ϵ_t is the current disturbance term. At each point in time, the information set upon which we condition the forecasts contains the actual values of the lagged endogenous variables and a random draw of the model parameters and hyperparameters. To calculate the conditional expectations, we randomly draw from the Gibbs sampler output at a given time t the time-varying coefficients, the variance covariance matrix and the hyperparameters. We employ the transition laws and stochastically simulate the future paths of the coefficient vector and the components of the variance covariance matrix for up to 20 quarters into the future. By projecting the evolution of the system we account for all potential three sources of uncertainty from the corresponding innovations in the system. To obtain the time t structural impact matrix, $B_{0,t}$ we first obtain a rotation matrix Q following (Rubio-Ramirez, Waggoner & Zha (2010)) and combine it with the lower triangular Cholesky factor of $\Omega_{t|T}$ resulting in $B_{0,t} = \Lambda_{t|T}^{-1}\Sigma_{t|T}Q'$. Given this contemporaneous impact matrix, we compute the reduced-form innovations based on the relationship $e_t = B_{0,t}\epsilon_t$. From the set of candidate impulse responses

derived in this way, only those satisfying our sign restriction are used to compute the impulse responses. All others are discarded. Based on these impulse responses, we calculate the statistics of interest. In particular, the minimum and maximum responses at each horizon are used to estimate the full identified set.

This procedure is computationally cumbersome and quite time consuming. We calculate the generalized impulse response functions at each point in time $t = 1, \ldots, 366$, given a random selection of 500 states of the economy explicitly taking into account possible future uncertainty in the structure of the economy along the horizon considered. For each of those random draws we calculate 50 candidate impulse response functions resulting in a total of 9.15 million candidates. The procedure described here (not including the Gibbs sampler to estimate the model in the reduced form model in the first place) takes for a given specification on an AMD Opteron(tm) Processor 6172, 2.10 GHz (8 processors), 16GB RAM and a 64-bit operating system about 7 days to run.

7 Drawing Measurement Errors and 'True' Data

This section describes the state space system used to generate draws of the measurement errors and the unobserved 'true' data. For notational convenience, we focus here on our benchmark specification, but generalizing this section to the case with general $M_i(L)$ is straightforward.

Let $S_t = (\mathbf{Y}_t, \mathbf{m}_t^1, \mathbf{m}_t^2, \mathbf{m}_t^3, \mathbf{m}_t^4, \mathbf{m}_t^5)'$ be the vector of unobserved data and measurement errors where $\mathbf{m}_t^i = (m_t^i, m_{t-1}^i, m_{t-2}^i, m_{t-3}^i, m_{t-4}^i)'$ for $i = 1, 2, 5$ where the index i denotes the measurement error associated with the VAR variable i in the ordering[6]. The joint state space representation for observed noisy data vector $\tilde{y}_t$ is defined as (we write the dynamics of $\mathbf{Y}_t$ as a VAR(1) - it is the companion form of our original VAR):

$$
\begin{aligned}
\tilde{y}_t &= J S_t \\
S_t &= \delta_t + F_t S_{t-1} + \omega_t
\end{aligned}
$$

where the state law of motion is given by the VAR and the measurement

---

[6]We could in principle include higher order lags of measurement errors for the interest rate and term spread for notational convenience. But in our application both variables are actually measured in levels.

error structure:

$$
\begin{bmatrix} \mathbf{Y}_t \\ \mathbf{m}_t^1 \\ \mathbf{m}_t^2 \\ m_t^3 \\ m_t^4 \\ \mathbf{m}_t^5 \end{bmatrix} = \begin{bmatrix} \mu_t \\ 0 \\ 0 \\ \vdots \\ 0 \end{bmatrix} + \begin{bmatrix} \mathbf{A}_t & 0 & \cdots & & & 0 \\ 0 & \rho_m^1 & 0 & & & \\ & 0 & \rho_m^2 & 0 & & \vdots \\ \vdots & & 0 & \rho_m^3 & 0 & \\ & & & 0 & \rho_m^4 & 0 \\ 0 & & \cdots & & 0 & \rho_m^5 \end{bmatrix} \begin{bmatrix} \mathbf{Y}_{t-1} \\ \mathbf{m}_{t-1}^1 \\ \mathbf{m}_{t-1}^2 \\ m_{t-1}^3 \\ m_{t-1}^4 \\ \mathbf{m}_{t-1}^5 \end{bmatrix} + \begin{bmatrix} \mathbf{e}_t \\ \varepsilon_t^{m,1} \\ \varepsilon_t^{m,2} \\ \varepsilon_t^{m,3} \\ \varepsilon_t^{m,4} \\ \varepsilon_t^{m,5} \end{bmatrix}
$$

where

$$
\rho_m^i = \begin{bmatrix} \rho_m^i & 0 & 0 & 0 & 0 \\ 1 & 0 & 0 & 0 & 0 \\ 0 & 1 & 0 & 0 & 0 \\ 0 & 0 & 1 & 0 & 0 \\ 0 & 0 & 0 & 1 & 0 \end{bmatrix}
$$

and $\varepsilon_t^{m,i} = (\varepsilon_t^{m,i}, 0, ..., 0)'$ for $i = 1, 2, 5$.

The covariance matrix of ω_t is given by

$$
Var(\omega_t) = \begin{bmatrix} Var(\mathbf{e}_t) & 0 & & \cdots & & & 0 \\ 0 & Var(\varepsilon_t^{m,1}) & 0 & & & & \\ & 0 & Var(\varepsilon_t^{m,2}) & 0 & & & \vdots \\ \vdots & & 0 & Var(\varepsilon_t^{m,3}) & 0 & & \\ & & & 0 & Var(\varepsilon_t^{m,4}) & 0 & \\ 0 & & \cdots & & 0 & Var(\varepsilon_t^{m,5}) \end{bmatrix}.
$$

Finally, the selection matrix J is specified such that

$$
\begin{bmatrix} \Delta gdp_t \\ \pi_t \\ i_t^s \\ spread_t \\ \Delta money_t \end{bmatrix} = \begin{bmatrix} y_{1,t} + m_t^1 - m_{t-4}^1 \\ y_{2,t} + m_t^2 - m_{t-4}^2 \\ y_{3,t} + m_t^3 \\ y_{4,t} + m_t^4 \\ y_{5,t} + m_t^5 - m_{t-4}^5 \end{bmatrix} = J \times S_t
$$

References

Balke, N. & Gordon, R. J. (1986), Appendix B Historical Data, *in* 'The American Business Cycle: Continuity and Change', NBER Chapters, National Bureau of Economic Research, Inc, pp. 781–850.

Baumeister, C. & Benati, L. (2013), 'Unconventional Monetary Policy and the Great Recession: Estimating the Macroeconomic Effects of a Spread Compression at the Zero Lower Bound', *International Journal of Central Banking* **9**(2), 165–212.

Baumeister, C. & Peersman, G. (2013), 'Time-Varying Effects of Oil Supply Shocks on the US Economy', *American Economic Journal: Macroeconomics* **5**(4), 1–28.

Benati, L. & Mumtaz, H. (2007), U.S. evolving macroeconomic dynamics: a structural investigation, Working Paper Series 0746, European Central Bank.

Bianchi, F. & Ilut, C. (2013), Monetary/fiscal policy mix and agents' beliefs, Technical report.

Carter, C. K. & Kohn, R. (1994), 'On gibbs sampling for state space models', *Biometrika* **81**(3), 541–553.

Cogley, T., Matthes, C. & Sbordone, A. (2015), 'Optimized taylor rules for disinflation when agents are learning', *The Journal of Monetary Economics, forthcoming* .

Cogley, T. & Sargent, T. J. (2005), 'Drift and volatilities: Monetary policies and outcomes in the post WWII U.S.', *Review of Economic Dynamics* **8**(2), 262–302.

Cogley, T., Sargent, T. J. & Surico, P. (2015), 'Price-level uncertainty and instability in the United Kingdom', *Journal of Economic Dynamics and Control* **52**(C), 1–16.

Kim, S., Shephard, N. & Chib, S. (1998), 'Stochastic volatility: Likelihood inference and comparison with ARCH models', *Review of Economic Studies* **65**(3), 361–93.

Koop, G., Pesaran, M. H. & Potter, S. M. (1996), 'Impulse response analysis in nonlinear multivariate models', *Journal of Econometrics* **74**(1), 119–147.

Primiceri, G. (2005), 'Time varying structural vector autoregressions and monetary policy', *Review of Economic Studies* **72**(3), 821–852.

Rubio-Ramirez, J. F., Waggoner, D. F. & Zha, T. (2010), 'Structural Vector Autoregressions: Theory of Identification and Algorithms for Inference', *Review of Economic Studies* **77**(2), 665–696.